Dissipative effects in the dynamics of N_2 on tungsten surfaces

2009 J. Phys.: Condens. Matter 21 264007

(http://iopscience.iop.org/0953-8984/21/26/264007)

J. Phys.: Condens. Matter **21** (2009) 264007 (6pp) doi:10.1088/0953-8984/21/26/264007

Dissipative effects in the dynamics of N_2 on tungsten surfaces

I Goikoetxea[1,2,3], J I Juaristi[1,2,3], M Alducin[3,4] and R Díez Muiño[3,4]

[1] Departamento de Física de Materiales, Facultad de Química, UPV/EHU, Apartado 1072, 20080 San Sebastián, Spain
[2] Centro de Física de Materiales Centro Mixto CSIC-UPV/EHU, Apartado 1072, 20080 San Sebastián, Spain
[3] Donostia International Physics Center DIPC, P Manuel de Lardizabal 4, 20018 San Sebastián, Spain
[4] Centro de Física de Materiales Centro Mixto CSIC-UPV/EHU, Edificio Korta, Avenida de Tolosa 72, 20018 San Sebastián, Spain

E-mail: wapjuoli@sq.ehu.es (J I Juaristi)

Received 31 October 2008, in final form 4 December 2008
Published 11 June 2009
Online at stacks.iop.org/JPhysCM/21/264007

Abstract

The role of electron–hole pair excitations in the dynamics of N_2 on W(100) and W(110) is evaluated using a theoretical model that accounts for the six-dimensionality of the problem in the whole calculation. The six-dimensional potential energy surface is determined in each case from an extensive grid of energies calculated with density functional theory. Dissipative effects due to electron–hole pair excitations are introduced in the classical dynamics equations through a friction force. Corresponding electron friction coefficients are calculated for each atom in the molecule with density functional theory in a local density approximation. Our results show that electronic friction plays a very minor role in the dissociative dynamics of N_2 in both tungsten faces. A similar conclusion is reached when we calculate the energy lost by the reflecting molecules.

(Some figures in this article are in colour only in the electronic version)

1. Introduction

State-of-the-art theoretical studies of elementary reactive processes of diatomic molecules at metal surfaces rely on the adiabatic Born–Oppenheimer approximation. These kinds of studies are based on a full six-dimensional (6D) calculation of the dynamics of the molecules on an *ab initio* potential energy surface (PES) that describes the molecule–surface interaction and neglects energy dissipation channels. Nevertheless, there exists experimental evidence that electronic excitations take place during the gas/surface reaction. For instance, electron–hole pair excitations are apparent in the detection of chemicurrents during the chemisorption of gas-phase species on thin metal films [1, 2], as well as in the measurement of electron emission following the scattering of molecules in highly excited vibrational states on metal surfaces [3, 4]. In principle, this fact puts into question the applicability of the adiabatic approach.

The contribution of electron–hole pair excitations to the dissociative adsorption has recently been evaluated in our group for two representative systems, N_2/W(110) and H_2/Cu(110) [5]. This was done by keeping the full six-dimensionality of the problem in the whole calculation: the potential energy surface, the friction force, and the dynamics ruled by these forces. The results showed that the contribution of electron excitations is a marginal correction to the adiabatic sticking probabilities.

In this work, we apply our theoretical method to the N_2/W(100) system and we compare the new results with those obtained previously for N_2/W(110). Dissociation of low-energy N_2 beams on W surfaces shows a strong sensitivity to the crystal face. While dissociation is considerable for vanishingly small beam energy on the W(100) surface [6, 7], it is roughly two orders of magnitude smaller at $T = 800$ K on the W(110) surface [8]. Adiabatic dynamics calculations performed on both surfaces explained this remarkable face sensitivity to dissociation [10]. In the N_2/W(100) case, the efficiency of dissociation at low energies was shown to be due to dynamic trapping: when approaching the surface, energy is transferred from translational motion to other degrees of

freedom so that the molecule cannot 'climb' back the potential slope toward the vacuum. In the case of N_2/W(110), dynamic trapping also plays the leading role at such low energies, but the low sticking coefficient is due to the low probability that molecules have of arriving at the precursor well. At high energies ($E > 400$ meV) dissociation takes place quite directly on both surfaces, since the kinetic energy allows the molecules to overcome the potential slopes without the need of being trapped by the potential well [11, 12]. Still, dissociation is also more effective on the W(100) surface, reflecting its sensitivity to the crystal face.

In view of these facts, it is interesting to investigate crystal face sensitivity to the frictional force. With this aim, we quantify in this work the effect of electronic friction on the dissociative dynamics of N_2 on W(100), and perform comparisons between the two crystal faces.

The organization of the paper is as follows. In section 2, we briefly describe the model employed to calculate the dissociative sticking coefficient of N_2 on W(100) and W(110). In section 3 the results of the calculation are presented and comparisons between the two faces are performed. Finally, in section 4 the main conclusions are summarized.

2. Theory

We perform 6D classical molecular dynamics simulations of the trajectories of N_2 molecules incident on the W surfaces. To model the molecule–surface interaction, we calculate the frozen 6D PES for the N_2/W(100) and N_2/W(110) systems, using density functional theory and the general gradient approximation with the Perdew–Wang energy functional (PW91) [13]. Details of the calculation and the set of configurations for which the *ab initio* energies are calculated can be found in [11] for the N_2/W(100) system and in [12] for the N_2/W(110) system. The energy grid consists of 3624 points for N_2/W(100) and of 5610 points for N_2/W(100). To perform the trajectory calculations we need to evaluate the 6D PES at any position $\mathbf{r}_i$ and $\mathbf{r}_j$ of the N atoms. Interpolation is then performed using the corrugation reducing procedure [14].

Nonadiabaticity is introduced by including electronic friction in the calculation of the classical trajectories of the molecule. The energy loss suffered by each of the N atoms is calculated independently. The basic quantity under study is the so-called electronic stopping power, which is the energy lost per unit path length or, in other words, the dissipative force experienced by the moving atom. The stopping power of slow atoms traveling through metals (projectile velocities lower than the Fermi velocity of the metal) has a linear dependence on velocity. This reflects the fact that in a metal there is no minimum energy required to excite electron–hole pairs. As a consequence, one can write the dissipative force entering the equations of the dynamics as the product of a friction coefficient η and the velocity of the atom $\mathbf{v}$:

$$\mathbf{F}_{\mathrm{diss}} = -\eta \mathbf{v}. \tag{1}$$

Therefore, the problem to be solved is the calculation of the friction coefficient along the trajectory for each atom in the molecule.

At low velocities an atom represents such a strong perturbation for the metal that perturbative treatments to calculate the friction coefficient are not justified. Alternatively, a well established approach based on density functional theory of screening and the kinetic theory of scattering for an atom moving in an electron gas has been successfully applied to the study of the energy loss of atoms and ions interacting with bulk metals [15–17] and their surfaces [18]. Here we adopt this model to calculate the friction coefficient. In the following we briefly describe the main ingredients of the model.

For low atom velocities the physics of atom–electron gas interaction occurs via scattering at the Fermi surface. As a consequence, the modulus of the dissipative force on the atom can be calculated in terms of the transport cross section at the Fermi level [15]:

$$F_{\mathrm{diss}} = n_0 v k_{\mathrm{F}} \sigma_{\mathrm{tr}}(k_{\mathrm{F}}), \tag{2}$$

where n_0 is the electron gas density, k_{F} the Fermi momentum and $\sigma_{\mathrm{tr}}(k_{\mathrm{F}})$ the transport cross section at the Fermi level. The product $k_{\mathrm{F}}\sigma_{\mathrm{tr}}(k_{\mathrm{F}})$ is the integrated scattering rate for momentum transfer which governs the dissipative process. Therefore, one can interpret the dissipative force described by equation (2) as the result of the momentum transfer per unit time to a uniform current of independent electrons ($n_0 v$) scattered by a fixed impurity potential. Note that, within this formalism, the friction coefficient in equation (1) reads $\eta = n_0 k_{\mathrm{F}} \sigma_{\mathrm{tr}}(k_{\mathrm{F}})$. The transport cross section is calculated to all orders in the nuclear charge of the atom in terms of the scattering phase-shifts at the Fermi level ($\delta_l(k_{\mathrm{F}})$):

$$\sigma_{\mathrm{tr}}(k_{\mathrm{F}}) = \frac{4\pi}{k_{\mathrm{F}}^2} \sum_{l=0}^{\infty} (l+1) \sin^2(\delta_l(k_{\mathrm{F}}) - \delta_{l+1}(k_{\mathrm{F}})). \tag{3}$$

In these equations the scattering potential is the screening potential induced by the impurity in the electron–gas system. We calculate this potential using density functional theory for an impurity embedded in an electron gas [19]. In this way, the model includes nonlinear effects both in the medium response to the atomic potential (nonlinear screening) and in the calculation of the relevant cross-section for the energy loss process. This is necessary in order to correctly represent the strong perturbation caused by the atomic particle and it is the reason behind the success of this model to describe the energy loss of slow atoms and ions in metals.

In order to obtain the energy lost through electron–hole pair excitations by the molecule, we first calculate the electronic density $n(\mathbf{r}_i)$ at each position $\mathbf{r}_i$ along the trajectory of the two N atoms. The surface electronic density $n(\mathbf{r}_i)$ is calculated *ab initio* and within the same conditions as the PES. The friction coefficient at each point of the trajectory is, subsequently, approximated by that corresponding to an electron gas with electronic density $n_0 = n(\mathbf{r}_i)$.

In summary, the classical equations of motion for each atom of the molecule that one has to solve read [5]

$$m_i \frac{\mathrm{d}^2 \mathbf{r}_i}{\mathrm{d}t^2} = -\nabla_i V(\mathbf{r}_i, \mathbf{r}_j) - \eta(\mathbf{r}_i) \frac{\mathrm{d}\mathbf{r}_i}{\mathrm{d}t}, \tag{4}$$

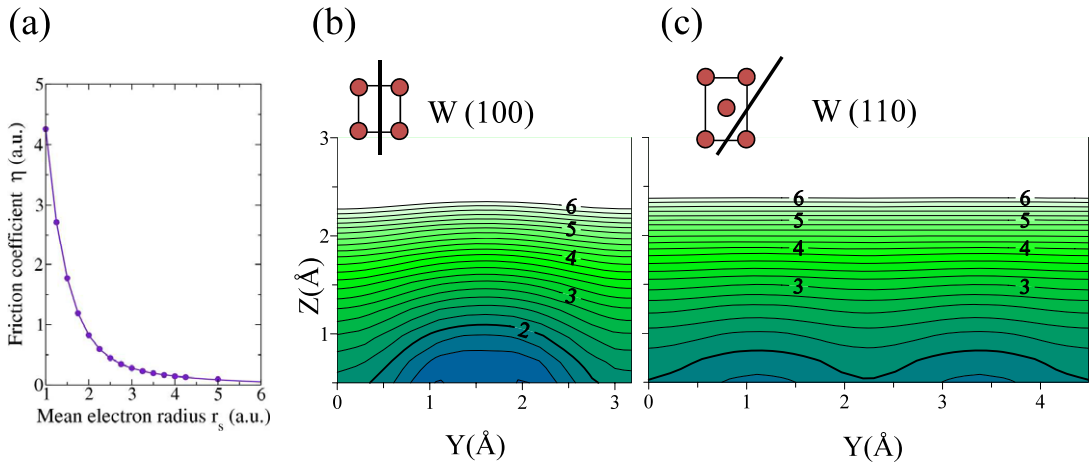

Figure 1. (a) Friction coefficient η for N in an electron gas as a function of the mean electron radius r_s. (b) Values of r_s for W(100) in a plane normal to the surface along the direction represented in the unit cell with a thick line. (c) Same for W(110).

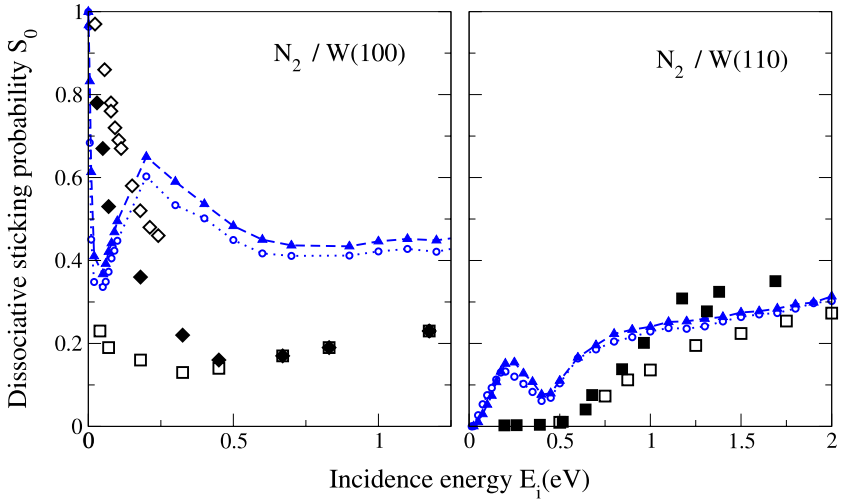

Figure 2. Dissociative sticking probability S_0 as a function of the incidence energy, for N_2 impinging on W(100) (left panel) and on W(110) (right panel). Filled blue triangles (open blue circles) are the results with (without) electronic friction. The experimental initial sticking coefficients of N_2 on the W(100) surface [6, 7] and on the W(110) surface [8, 9] are also shown for comparison in each panel. Surface temperature is 800 K (white squares), 300 K (black diamonds), and 100 K (white diamonds) for W(100), and 800 K (white and black squares) for W(110).

where the first term on the right-hand side is the adiabatic force obtained from the 6D PES $V(\mathbf{r}_i, \mathbf{r}_j)$ and the second term is the dissipative force experienced by each atom in the molecule. The results of the adiabatic calculation that we show are obtained by neglecting the dissipative force.

3. Results

The dissociative dynamics of N_2 on W(100) and on W(110) are respectively studied in detail in [11] and [12] using the adiabatic approximation. Here we apply our theoretical approach to analyze and compare the role of electronic friction in the reactivity of N_2 on both surfaces. Figure 1(a) shows the friction coefficient η for the N atom inside an electron gas as a function of the mean electron radius r_s. The latter is defined from the electron gas density n_0 as $r_s = [3/(4\pi n_0)]^{1/3}$. Also in figure 1, we show the r_s values in a plane normal to the surface for (b) W(100) and (c) W(110). In each case, the cutting plane is oriented along the direction indicated by a straight line on the respective surface unit cell. These orientations are representative of the positions of the dissociating N_2 at $Z \leqslant 1.5$ Å (see [11, 12]). Note that, comparing the depicted 2D cuts, the electron density is more corrugated on the W(100) surface at these distances.

The dissociative sticking probabilities of N_2 with and without including electronic friction are compared in figure 2 for both tungsten surfaces. Probabilities are represented as a function of the incidence energy E_i. All the results shown in this work are calculated for normal incidence conditions. The reactive probabilities are derived from a minimum of 5000 trajectories using a conventional Monte Carlo sampling of all possible initial conditions. We perform pure classical dynamics calculations of the trajectories, i.e.,

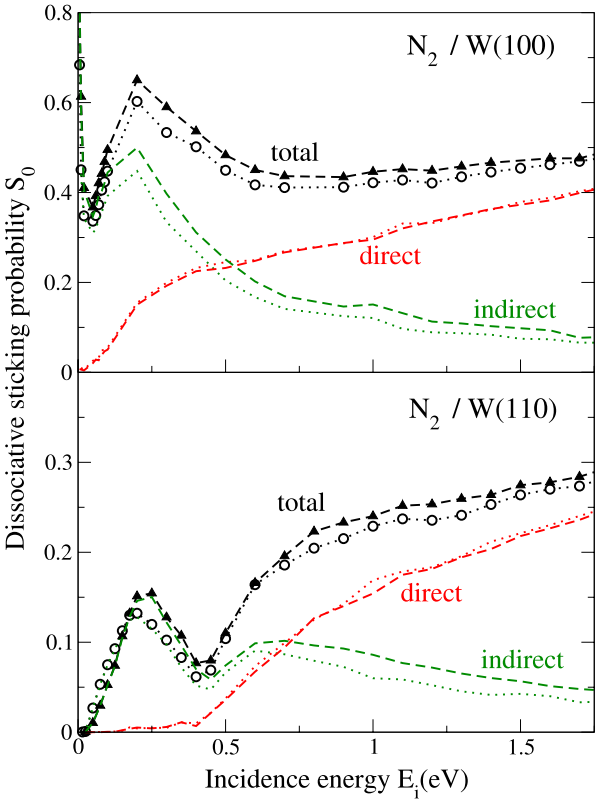

Figure 3. Dissociative sticking probability S_0 as a function of the incidence energy, for N_2 impinging on W(100) (upper panel) and on W(110) (lower panel). Full triangles (open circles) are the results with (without) electronic friction. Contributions to S_0 coming from the direct and the indirect channels are also represented. Dashed and dotted curves show the results with and without including electronic friction, respectively.

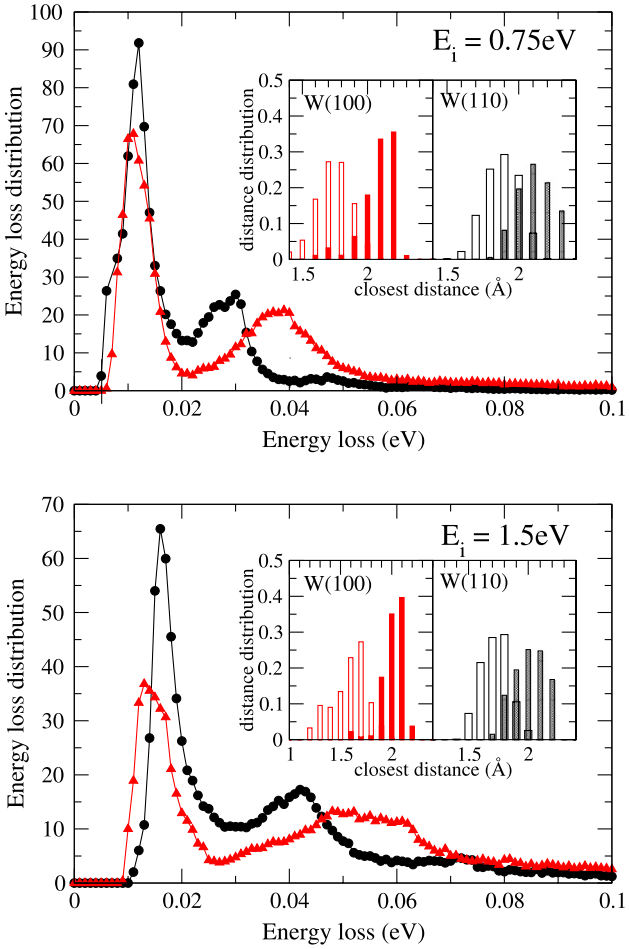

Figure 4. Energy loss spectra of the N_2 molecules reflected from W(110) (full black circles) and W(100) (full red triangles). The insets show the closest approach distance distribution of those reflecting molecules that contribute to the low-energy (shadowed bars) and high-energy (open bars) loss peaks (see footnote 5). Incidence energies are $E_i = 0.75$ eV (upper panel and the two insets) and $E_i = 1.5$ eV (lower panel and the two insets).

the initial zero-point energy of N_2 is neglected. In general, the dissociative sticking probability increases when electronic friction is included. Corrections are however very minor for both surfaces and amount up to a maximum of about 10% in a large range of energies. In any case, the inclusion of electron–hole pair excitations do not improve the comparison between theoretical simulations and experimental data.

Under normal incidence conditions, the analysis of the adiabatic trajectories performed in [11, 12] shows that dissociation proceeds either through a direct or an indirect mechanism. In the former, dissociation takes place after no or a very small number of rebounds n_{reb}. In the latter, molecules are dynamically trapped close to the surface, bouncing off several times before dissociating. We find that the effect of including friction is to increase the indirect mechanism. This is observed in figure 3 by comparing the results obtained with and without including electronic friction. In this figure, the direct channel corresponds to $n_{\mathrm{reb}} < 4$ and the indirect one to $n_{\mathrm{reb}} \geqslant 4$. Whereas the direct channel remains almost unchanged, there is an increase in the indirect one that practically coincides with that observed in the total dissociation probability. We have verified that this observation is independent of the n_{reb} value chosen to distinguish between the direct and the indirect mechanisms, provided that it is reasonably selected to define direct dissociation.

The important conclusion of our calculations is that the effect of electronic friction in the dissociative dynamics is very minor. The reason to understand this marginal role is the following. Although the friction coefficients can be large, this is not enough to infer an energy loss that will affect the dynamics in a significant way. The dissipative force is proportional to the friction coefficient and the projectile velocity. In the region where the electron density is high, the molecule–surface potential is highly repulsive. As a consequence, the kinetic energy of the molecules is substantially reduced. This is what makes the dissipative force small and what makes the energy loss a marginal effect.

The analysis of the reflected molecules can provide quantitative information on the role of electronic friction in the interaction of low-energy molecules with metal surfaces. In figure 4, we show the energy loss distribution of the reflected molecules with an initial incidence energy $E_i = 0.75$ eV (upper panel) and $E_i = 1.5$ eV (lower panel). In all cases, the energy lost due to electronic friction is very small, though it might be measured with present experimental

techniques. Note, however, that phonon excitations and surface temperature not included in present calculations will modify the spectra. The two peak structure can be related to the distances of closest approach to the surface Z_{min} probed by the reflected molecules. As a general trend, molecules contributing to the high-energy loss peak probe distances close to the surface, where the electronic density is high. In contrast, the low-energy peaks correspond to molecules that are reflected at larger distances from the surface. This can be observed in the insets of figure 4, which show the Z_{min} distributions for the trajectories that give rise to the low-energy loss peaks (shadow bars) and for the ones that give rise to the high-energy loss peaks (open bars)[5]. Furthermore, another different feature between the molecules contributing to the low- and high-energy peaks is related to the number of rebounds. Molecular trapping is almost negligible in the reflection process at these incidence energies: most molecules are reflected after one rebound at most. Still, there are a small number of molecules that show two to four rebounds before being finally reflected. We find that only about 0.1% of the molecules contributing to the low-energy peak show more than one rebound. This percentage substantially increases for the molecules contributing to the high-energy peak, in particular for those reflected from the W(100) surface[6]. The correlation between number of rebounds and energy loss also allows us to rationalize the fact that the latter peak is at higher energies for the W(100) surface, since a larger number of rebounds is expected to imply a longer interaction time.

Additionally, we verify that the average energy lost by the reflected N_2 constitutes a low percentage of the initial kinetic energy. Results are represented in figure 5 for both surfaces. The inset shows the average number of rebounds of the reflecting molecules as a function of the incidence energy. We observe that the energy loss is slightly higher when molecules are reflected from the W(100) surface. As shown in the inset, this is again consistent with a larger number of rebounds, since the molecules stay longer in contact with the surface and, therefore, can lose more energy.

Finally, we would like to remark that our results show the low efficiency of electron–hole pair excitations as an energy loss channel for the reflected molecules. If higher energy losses were measured, they should be attributed to different dissipation mechanisms such as phonon excitations.

4. Conclusions

In summary, we have studied dissipative effects due to electron–hole pair excitations in the dynamics of N_2 interacting with W(100) and W(110). Our theoretical model preserves the six-dimensionality of the problem in the potential energy surface and in the calculations that incorporate electronic dissipation through a friction force. Calculations with and without including electronic friction allow us to quantify the role of nonadiabaticity in the dissociative dynamics of N_2/W(100) and N_2/W(110). Electronic friction increases the indirect channel to dissociation and does not affect the direct one. Nevertheless, our results show that the contribution of electron excitations is a marginal correction and, therefore, that an adiabatic calculation is meaningful to calculate the dissociative sticking coefficient in these two surfaces. Additionally, we have calculated the energy loss of the reflected N_2 molecules at both surfaces, and show that the energy loss is only a few per cent of the initial energy in both cases. The low velocity of the reacting molecules in the surface regions of high electronic density is the main reason to explain these facts. Regarding the comparison between the two surfaces, higher energy losses are expected for molecules reflected at the W(100) surface, due to a larger number of trajectories that suffer rebounds in this surface before reflection, which implies a longer interaction time.

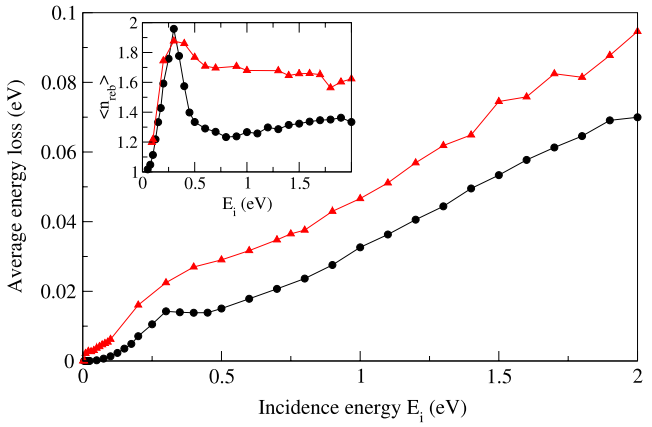

Figure 5. Average-energy loss of reflecting N_2 molecules scattered from W(110) (full black circles) and from W(100) (full red triangles) as a function of the incidence energy. The average number of rebounds is represented in the inset for both cases.

Acknowledgments

We acknowledge partial support by the Spanish MCyT (grant No FIS2007-066711-CO2-00). Computational resources were provided by the Donostia International Physics Center and the SGI/IZO-SGIker at the UPV/EHU (supported by the Spanish Ministry of Education and Science and the European Social Fund).

References

[1] Gergen B, Nienhaus H, Weinberg W H and McFarland E W 2001 *Science* **294** 2521
[2] Krix D, Nünthel R and Nienhaus H 2007 *Phys. Rev.* B **75** 073410
[3] Huang Y, Rettner C T, Auerbach D J and Wodtke A M 2000 *Science* **290** 111
[4] White J D, Chen J, Matsiev D, Auerbach D J and Wodtke A M 2005 *Nature* **433** 503

[5] Energy limits used in this analysis to define the low- and high-energy loss peaks. For W(100) and $E_i = 0.75$ eV: 5–17 and 25–50 meV. For W(100) and $E_i = 1.5$ eV: 9–25 and 40–70 meV. For W(110) and $E_i = 0.75$ eV: 5–17 meV and 20–40 meV. For W(110) and $E_i = 1.5$ eV: 10–25 and 35–55 meV.

[6] The percentage of molecules contributing to the high-energy loss peak that show more than one rebound is 63% for $E_i = 0.75$ eV and 24% for $E_i = 1.5$ eV on the W(100) surface; and 30% for $E_i = 0.75$ eV and 6% for $E_i = 1.5$ eV on the W(110) surface.

[5] Juaristi J I, Alducin M, Díez Muiño R, Busnengo H F and Salin A 2008 *Phys. Rev. Lett.* **100** 116102
[6] Rettner C T, Schweizer E K, Stein H and Auerbach D J 1988 *Phys. Rev. Lett.* **61** 986
[7] Rettner C T, Stein H and Schweizer E K 1988 *J. Chem. Phys.* **89** 3337
[8] Pfnür H E, Rettner C T, Lee J, Madix R J and Auerbach D J 1986 *J. Chem. Phys.* **85** 7452
[9] Rettner C T, Schweizer E K and Stein H 1990 *J. Chem. Phys.* **93** 1492
[10] Alducin M, Díez Muiño R, Busnengo H F and Salin A 2006 *Phys. Rev. Lett.* **97** 056102
[11] Volpilhac G and Salin A 2004 *Surf. Sci.* **556** 129
[12] Alducin M, Díez Muiño R, Busnengo H F and Salin A 2006 *J. Chem. Phys.* **125** 144705
[13] Perdew J P, Chevary J A, Vosko S H, Jackson K A, Pederson M R, Singh D J and Fiolhais C 1992 *Phys. Rev.* B **46** 6671
[14] Busnengo H F, Salin A and Dong W 2000 *J. Chem. Phys.* **112** 7641
[15] Echenique P M, Nieminen R M and Ritchie R H 1981 *Solid State Commun.* **37** 779
[16] Echenique P M, Nieminen R M, Ashley J C and Ritchie R H 1986 *Phys. Rev.* A **33** 897
[17] Alducin M, Díez Muiño R, Juaristi J I and Echenique P M 2002 *Phys. Rev.* A **66** 054901
[18] Juaristi J I, Arnau A, Echenique P M, Auth C and Winter H 1999 *Phys. Rev. Lett.* **82** 1048
[19] Zaremba E, Sander L M, Shore H B and Rose J H 1977 *J. Phys. F: Met. Phys.* **7** 1763